

Effect of inhaled nitric oxide on intestinal integrity in cardiopulmonary bypass and circulatory arrest simulation: An experimental study

Address for correspondence:
Dr. Nikolay O. Kamenshchikov,
Cardiology Research Institute,
Tomsk NRCM, 111a Kievskaya
Str., Tomsk, 634012, Russian
Federation.
E-mail: nikolajkamenof@mail.ru

Submitted: 28-Dec-2023

Revised: 14-Apr-2024

Accepted: 25-Apr-2024

Published: 07-Jun-2024

**Nikolay O. Kamenshchikov¹, Elena A. Churilina¹, Vyacheslav A. Korepanov²,
Tatiana Y. Rebrova², Irina V. Sukhodolo³, Boris N. Kozlov¹**

¹Laboratory of Critical Care Medicine, Cardiology Research Institute, Tomsk National Research Medical Center, Russian Academy of Sciences, 111a Kievskaya St., Tomsk 634012, ²Laboratory of Molecular and Cellular Pathology and Gene Diagnostics, Cardiology Research Institute, Tomsk National Research Medical Center, Russian Academy of Sciences, 111a Kievskaya St., Tomsk 634012, Russian Federation, ³Department of Morphology and General Pathology, Siberian State Medical University, 2 Moskovsky trakt, Tomsk, 634050, Russian Federation

ABSTRACT

Background and Aims: Cardiopulmonary bypass (CPB) and circulatory arrest (CA) can induce intestinal injury and consequently lead to multiple organ dysfunction. Nitric oxide (NO) has protective effects, but its effect on the intestine has not been studied. The study aimed to investigate intestinal injury variables and prove the intestinal protective effects of exogenous nitric oxide when modelling CPB and CA in an experiment. **Methods:** The study was performed on sheep ($n = 24$). There were four groups: CPB, CPB + NO, CPB + CA and CPB + CA + NO. Sheep in NO groups received intraoperative inhalation of NO at a dose of 80 ppm. Groups without NO underwent CPB and CA without NO delivery. Defaecation rate, dynamics of intestinal fatty acid binding protein (i-FABP), coefficient of microviscosity and polarity in the areas of lipid–lipid and protein–lipid interactions of erythrocyte membranes were assessed. One hour after CPB, the intestinal tissue was collected and assessed for tissue concentrations of adenosine triphosphate (ATP) and lactate. **Results:** The defaecation rate after CPB was higher in the CPB + NO group than in the CPB group. The concentration of i-FABP after CPB was lower in the CPB + NO and CPB + CA + NO groups than in the CPB and CPB + CA groups. Erythrocyte deformability before and after CPB revealed no significant dynamics in groups with NO. The ATP concentration 1 h after CPB was higher in the CPB + NO group than in the CPB group. The morphological picture in groups with NO was better. **Conclusion:** When modelling CPB and CA, NO had a positive effect on the functional and structural state of the intestine and also maintained erythrocyte deformability.

Keywords: Cardiopulmonary bypass, circulatory arrest, erythrocyte deformability, intestine, intestines, nitric oxide

Access this article online
Website: https://journals.lww.com/ijaweb
DOI: 10.4103/ija.ija_1267_23
Quick response code


INTRODUCTION

Cardiopulmonary bypass (CPB) and circulatory arrest (CA) lead to the development of ischaemia–reperfusion injury. This is associated with subclinical damage to the gastrointestinal tract, disruption of the integrity of the intestinal wall and translocation of microbiota into the systemic bloodstream, which is the engine of multiple organ failure.^[1-3] Perioperative delivery of nitric oxide (NO) is a promising method of organ protection.^[4,5] The study aimed to investigate intestinal injury variables and prove the intestinal

protective effects of exogenous NO when modelling CPB and CA in an experiment.

This is an open access journal, and articles are distributed under the terms of the Creative Commons Attribution-NonCommercial-ShareAlike 4.0 License, which allows others to remix, tweak, and build upon the work non-commercially, as long as appropriate credit is given and the new creations are licensed under the identical terms.

For reprints contact: WKHLRPMedknow_reprints@wolterskluwer.com

How to cite this article: Kamenshchikov NO, Churilina EA, Korepanov VA, Rebrova TY, Sukhodolo IV, Kozlov BN. Effect of inhaled nitric oxide on intestinal integrity in cardiopulmonary bypass and circulatory arrest simulation: An experimental study. *Indian J Anaesth* 2024;68:623-30.

METHODS

A single-centre, randomised, controlled experimental study of the effect of NO on the intestine was conducted under simulated CPB and CPB + CA conditions. All procedures were carried out in a testing laboratory in accordance with international standards for the humane treatment of laboratory animals and Directive 2010/63/EU of the European Parliament and the Council of 22 September 2010 on the protection of animals used for scientific purposes. The experiment was carried out in the laboratory of critical care medicine after obtaining approval from the local biomedical ethics committee of the Cardiology Research Institute (approval No. 230, dated 28 June 2022).

Randomisation by generating random numbers and allocation concealment were done using sequentially numbered opaque envelopes ($n = 24$). A research assistant who was not involved in the experimental study prepared, numbered and opened the envelopes on the day of the study; he also numbered the test tubes for collecting samples and took them to the laboratory. Each envelope was numbered from 1 to 24. A group of anaesthesiologists, cardiac surgeons and perfusionists performed the entire experiment. They were informed of the data inside the envelopes in the morning before the start of the experiment. Laboratory and histological analyses were carried out by other assistants, who were given samples with the experiment number. They were not aware of which group of animals it was.

The object of the study was Altai breed sheep weighing 30–34 kg. The experimental animals were randomised into four groups of six sheep in each group - NO under CPB, NO under CPB + CA, standard CPB or CPB + CA protocol in a 1:1:1:1 ratio. In the CPB and CPB + CA groups, a standard technique for conducting mechanical ventilation and CPB was carried out according to the protocol regulated by current clinical guidelines. In the CPB + NO group, the delivery of inhaled NO began after intubation through a ventilator circuit throughout the experiment at a concentration of 80 ppm. After the start of CPB, NO was delivered through an extracorporeal circulation circuit for 90 min; after weaning from CPB and returning to spontaneous circulation, the supply of NO continued through a circuit of the ventilator at a concentration of 80 ppm for 1 h. In the CPB + CA + NO group, delivery of inhaled NO began immediately after

tracheal intubation through a ventilator circuit at a concentration of 80 ppm. Then, after the start of CPB, NO delivery was carried out through a modified extracorporeal circulation circuit until the start of hypothermic CA. CA was performed by clamping the thoracic aorta while maintaining perfusion of the upper body and reducing the perfusion index to 1 l/min/m² for 15 min; NO delivery was not performed during CA. Upon CA completion, NO delivery was resumed until the end of the study.

The experiment in all groups began with mask induction of anaesthesia with sevoflurane. The animal's surgical field was prepared upon achieving the desired level of anaesthesia. The great saphenous vein of the hind limb was catheterised for the infusion therapy. Premedication included atropine sulphate 0.5 mg and chlorpyramine 20 mg. Before induction of anaesthesia, pulse oximetry and electrocardiography (ECG) were monitored continuously. Next, induction anaesthesia was performed with propofol 1% until signs of anaesthesia appeared, followed by intubation with an endotracheal tube of size 6.5 mm internal diameter. Mechanical ventilation was started using the Puritan Bennett 760 (USA) device with a tidal volume of 8 ml/kg, respiratory rate of 20 breaths per minute, fractional oxygen concentration in the inhaled mixture of 0.5 and a positive end-expiratory pressure of 5 cm H₂O. Throughout the experiment, propofol 5 mg/kg/h was infused to maintain anaesthesia and pipercuronium bromide 0.1 mg/kg was administered to provide neuromuscular blockade. Extended monitoring included ECG, invasive measurement of blood pressure (BP), pulse oximetry, capnography and thermometry using the Nihon Kohden Life Scope I BSM-2301 K monitoring system (Nihon Kohden, Tokyo, Japan), as well as diuresis.

For invasive measurement of BP, collection of blood samples and infusive therapy, the common carotid artery and the internal jugular vein were surgically harvested and catheterised. The blood gas composition, acid-base balance, haematocrit levels, electrolyte, lactate, glucose, haemoglobin and methaemoglobin concentrations were assessed with STAT PROFILE Critical Care Xpress analyser (Nova Biomedical, Waltham, MA, USA) in all groups before CPB, after CPB and 1 h after CPB. Next, a right thoracotomy was performed along the fourth intercostal space. CPB was performed using a CPB machine, Maquet HL 20 (Maquet, Rastatt, Germany). The CPB machine was connected according to the 'aorta–superior vena cava–inferior vena cava' scheme.

During CPB, the perfusion index was 2.5 l/min/m². Mean BP during CPB was maintained at 50–60 mmHg. In two groups with CA, upon reaching the oesophageal temperature of 30°C, occlusion of the thoracic aorta was performed for 15 min. After 15 min, the thoracic aorta was unclamped, followed by reperfusion and warming to 36.6°C. Heparin was used intravenously at a 3 mg/kg to ensure hypercoagulation during CPB, maintaining an activated clotting time >450 s. (A detailed description of the methods of anaesthesia and CPB is available in the Online Supplement.)

For NO delivery and NO/NO₂ monitoring, we used a special device for plasma-chemical NO synthesis AIT-NO-01 ('Tianox'), manufactured by the Russian Federal Nuclear Center – All-Russian Research Institute of Experimental Physics (Rosatom State Corporation Enterprise, Sarov, Russia). The maximum permissible NO₂ concentration was considered 2 ppm. (A detailed description of the method of delivering NO to the ventilator and CPB circuits is available in the Online Supplement.)

The endpoints for a comprehensive assessment of the severity of intestinal injury during CPB and hypothermic CA were defaecation rate (g/h) before CPB, after CPB and 1 h after CPB, the marker of intestinal ischaemia – intestinal enterocyte fatty acid binding protein (i-FABP) before and after CPB, coefficient of microviscosity in the areas of lipid–lipid (CMLLI) and protein–lipid interactions (CMPLI) of erythrocyte membranes, and coefficient of polarity in the areas of lipid–lipid (CPLLI) and protein–lipid interactions (CPPLI) of erythrocyte membranes before and after CPB. Histological examination was performed in intestinal biopsies and tissue concentrations of adenosine triphosphate (ATP) and lactate were determined 1 h after CPB. (A detailed description of the analysis of the obtained endpoints is available in the Online Supplement.)

Statistical analysis was performed using the Statistica software, version 12.0.0.0 (StatSoft, Tulsa, OK, USA). The normality test was carried out using the Shapiro–Wilk test. Mean (M) and standard deviation (SD) were used. To identify significant differences in quantitative variables in dependent groups at the stages of the study and independent groups for comparison between the CPB and CPB + NO, CPB + CA, and CPB + CA + NO groups, the Student's *t*-test was used. All statistical analysis results were considered statistically significant at a threshold significance level of $P = 0.05$.

RESULTS

The defaecation rate after CPB in the CPB + NO group was higher than in the CPB group ($P = 0.046$) [Table 1; Figure 1a and b].

The concentration of i-FABP in the CPB + NO and CPB + CA + NO groups after CPB was significantly lower than in the CPB and CPB + CA groups in pairwise comparison ($P = 0.002$ and $P = 0.033$, respectively) [Table 2; Figure 2a].

The mean (SD) ATP concentrations in intestinal biopsies 1 h after CPB were as follows: CPB group: 4.18 (0.23) [95% confidence interval (CI): 0.15, 0.58] nmol/g; CPB + NO group: 6.10 (1.31) [95% CI: 0.82, 3.22] nmol/g; CPB + CA group: 3.59 (0.50) [95% CI: 0.31, 1.24] nmol/g; CPB + CA + NO group: 2.96 (1.00) [95% CI: 0.63, 2.47] nmol/g. The ATP concentration was higher in the CPB + NO group than in the CPB group ($P = 0.005$) [Figure 2b].

The mean (SD) lactate concentration in the intestinal tissue 1 h after CPB was as follows: CPB group: 10.21 (2.48) [95% CI: 1.55, 6.09] mmol/g; CPB + NO group: 8.88 (3.63) [95% CI: 2.27, 8.91] mmol/g; CPB + CA group: 11.32 (0.78) [95% CI: 0.49, 1.92] mmol/g; CPB + CA + NO group: 10.70 (2.89) [95%

Table 1: Dynamics of defaecation rate at different stages of the study: before CPB, after CPB, 1 h after CPB

Defaecation rate (g/h) at different stages of the study in CPB and CPB + NO groups				
Variables	Stages	CPB group	CPB + NO group	<i>P</i>
Defaecation rate	Before CPB	133.5 (10.09) [6.3-24.76]	131.33 (8.01) [5.01-19.66]	0.689
	After CPB	45.0 (9.25) [5.78-22.69]	56.33 (8.04) [5.02-19.72]	0.046
	1 h after CPB	3.16 (2.78) [1.74-6.83]	3.83 (2.31) [1.45-5.68]	0.661
Defaecation rate (g/h) at different stages of the study in CPB + CA and CPB + CA + NO groups				
Variables	Stages	CPB + CA group	CPB + CA + NO group	<i>P</i>
Defaecation rate	Before CPB	124.66 (8.26) [5.16-20.26]	132.16 (10.72) [6.69-26.29]	0.204
	After CPB	42.66 (9.91) [6.19-24.31]	52.166 (7.13) [4.46-17.51]	0.086
	1 h after CPB	1.50 (1.76) [1.09-4.32]	3.00 (2.52) [1.58-6.21]	0.260

Data expressed as mean (standard deviation) [95% confidence interval]. CA=circulatory arrest, CPB=cardiopulmonary bypass, NO=nitric oxide

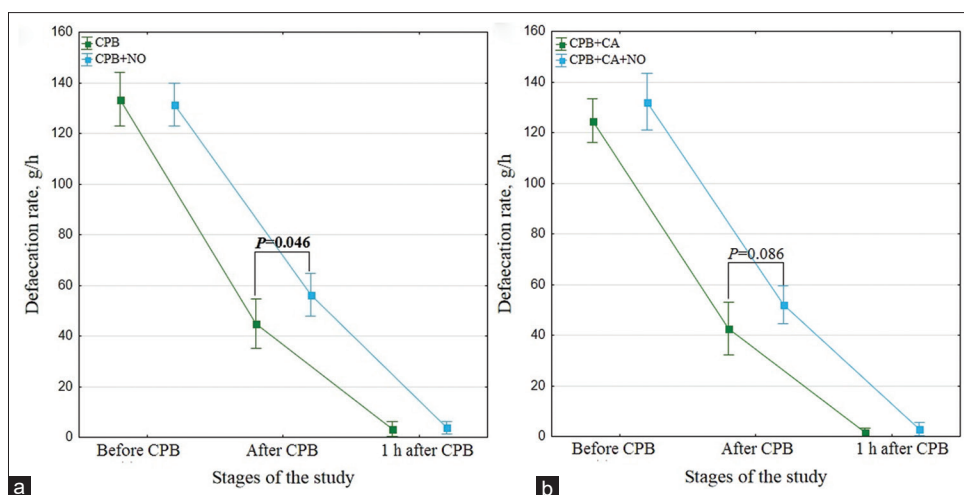


Figure 1: (a) Dynamics of defaecation rate in CPB and CPB + NO groups at different stages of the study; (b) dynamics of defaecation rate in CPB + CA and CPB + CA + NO groups at different stages of the study. CA = circulatory arrest, CPB = cardiopulmonary bypass, NO = nitric oxide

Table 2: Dynamics of i-FABP concentration before CPB and after CPB

i-FABP (pg/ml) in CPB and CPB + NO groups				
Variables	Stages	CPB group	CPB + NO group	P
i-FABP	Before CPB	11.27 (2.85) [1.78-7.01]	10.73 (1.73) [1.08-4.25]	0.698
	After CPB	62.79 (14.79) [9.23-36.28]	33.23 (10.38) [6.48-25.48]	0.002
i-FABP (pg/ml) in CPB + CA and CPB + CA + NO groups				
Variables	Stages	CPB + CA group	CPB + CA + NO group	P
i-FABP	Before CPB	11.89 (4.11) [2.57-10.09]	10.19 (3.63) [2.27-8.92]	0.466
	After CPB	60.42 (9.24) [5.77-22.69]	43.41 (14.13) [8.82-34.66]	0.033

Data expressed as mean (standard deviation) [95% confidence interval]. CA=circulatory arrest, CPB=cardiopulmonary bypass, i-FABP=intestinal enterocyte fatty acid binding protein, NO=nitric oxide

CI: 1.80, 7.08] mmol/g. There were no statistically significant differences in lactate concentration between CPB and CPB + NO, CPB + CA and CPB + CA + NO groups ($P = 0.476$ and $P = 0.506$, respectively).

A microscopic picture of the small intestinal tissue is shown in Figure 3a–d.

In the CPB group, a generalised oedema of all membranes of the small intestine was expressed. There was severe hyperemia of the intestinal villus capillaries, submucosal and intermuscular nerve plexuses and venous plethora of submucosa [Figure 3a].

In the CPB + NO group, all membranes of the small intestine had a normal appearance. The central lymphatic capillary of the intestinal villi in all parts of the intestine was expanded in the upper third, which was why the intestinal villi looked club-shaped. Moderate hyperemia of the submucosal vessels was noticeable [Figure 3b].

In the CPB + CA group, the lumen of the small intestine was filled with desquamated epithelial cells and single

cells with round nuclei. Intestinal villi were necrotic, and intestinal crypts were intact and infiltrated with round nuclei cells. There was a generalised oedema of all membranes of the small intestine [Figure 3c].

In the CPB + CA + NO group, there was moderate hyperemia of the vessels of the submucosa. Intestinal villi were necrotic; intestinal crypts were intact and infiltrated with round nuclei cells. There was generalised oedema of all membranes of the small intestine [Figure 3d].

Thus, it was found that in the CPB + NO and CPB + CA + NO groups, signs of hypoperfusion intestinal injury were less pronounced than in the CPB and CPB + CA groups.

Table 3 presents data on the dynamics of the coefficient of microviscosity and polarity in the areas of lipid–lipid and protein–lipid interactions of erythrocyte membranes.

When analysing CMPLI in the CPB group after CPB, a significant decrease from the initial values was

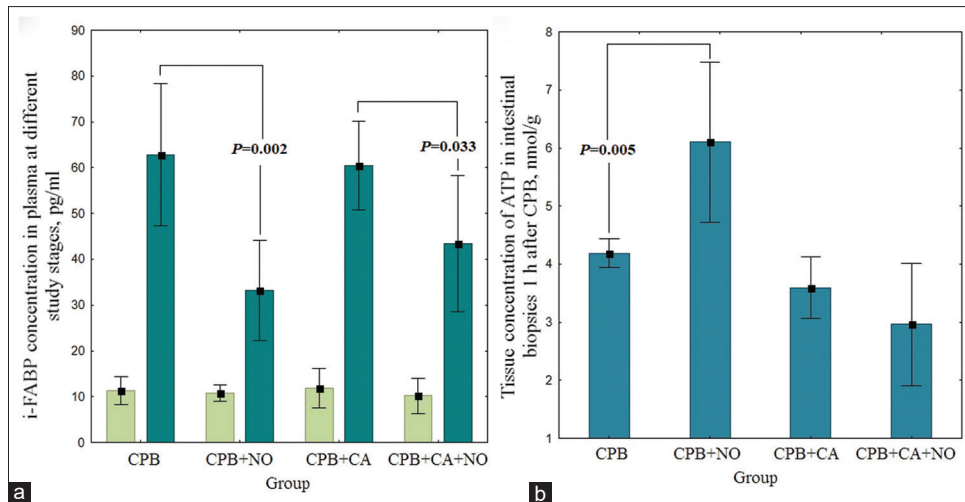


Figure 2: (a) Dynamics of i-FABP concentration at different stages of the study in CPB and CPB + NO, CPB + CA and CPB + CA + NO groups; (b) tissue concentration of ATP in intestinal biopsies 1 h after weaning from CPB in CPB and CPB + NO, CPB + CA and CPB + CA + NO groups. ATP = adenosine triphosphate, CA = circulatory arrest, CPB = cardiopulmonary bypass, iFABP = intestinal fatty acid binding protein, NO = nitric oxide

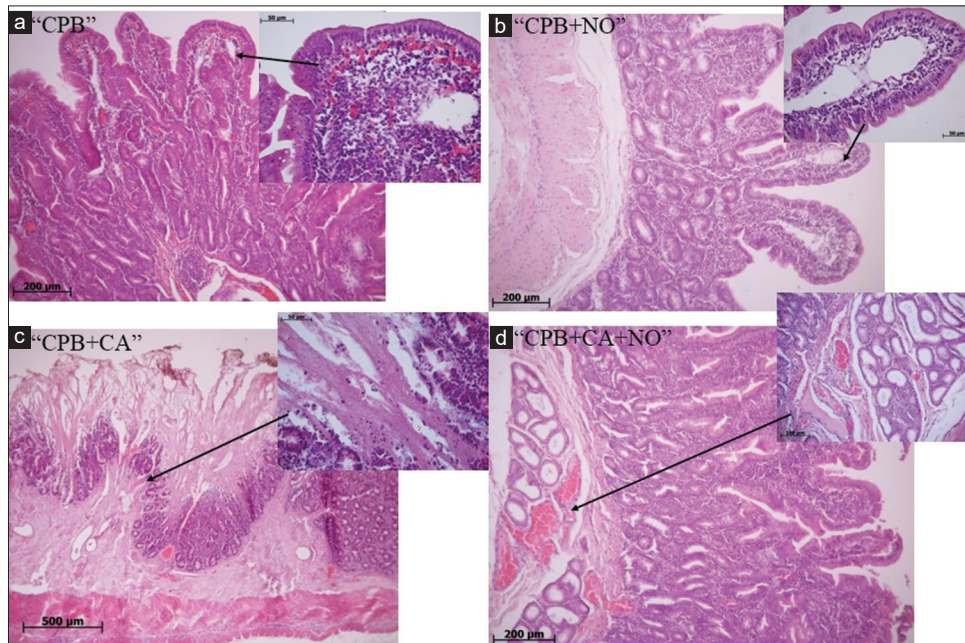


Figure 3: Histology of the small intestine $\times 500$, $\times 200$, $\times 100$, $\times 50$ stained with haematoxylin and eosin in groups: (a) CPB, (b) CPB + NO, (c) CPB + CA and (d) CPB + CA + NO. CA = circulatory arrest, CPB = Cardiopulmonary bypass, NO = nitric oxide

found ($P = 0.009$). In the CPB + NO group, there were no changes in CMPLI at the observation stages of the study. When analysing CPPLI in the CPB group after CPB, a significant decrease from the initial values was found ($P = 0.013$). In the CPB + NO group, no changes in CPPLI were recorded after CPB compared to the initial values. There was a decrease in CMPLI compared to the initial values in the CPB + CA group after CPB ($P = 0.049$). In the CPB + CA + NO group, no changes were detected in CMPLI at the observation stages of the study. There was a decrease in CPPLI compared to the initial values in the CPB + CA group

after CPB ($P = 0.022$). In the CPB + CA + NO group, no changes were detected in CPPLI at the observation stages of the study.

DISCUSSION

Our findings indicate that exogenous delivery of NO during CPB and CA leads to an improvement in the intestine's functional state, a decrease in the concentration of organ injury markers and an increase in ATP concentration and also has a positive effect on the structural organisation of erythrocyte membranes

Table 3: Coefficient of microviscosity and polarity of erythrocyte membranes at the observation stages: before CPB and after CPB in CPB and CPB + NO groups, CPB + CA and CPB + CA + NO groups, M (SD) [95% CI]

Coefficient of microviscosity and polarity of erythrocyte membranes at the observation stages in CPB and CPB + NO groups						
Variables	Stages	CPB group	P (between the stages of before and after CPB)	CPB + NO group	P (between the stages of before and after CPB)	P (between groups)
CMLLI	Before CPB	0.29 (0.11) [0.07-0.27]	0.741	0.26 (0.12) [0.07-0.29]	0.885	0.668
	After CPB	0.28 (0.10) [0.06-0.25]		0.25 (0.03) [0.02-0.06]		0.520
CMPLI	Before CPB	0.40 (0.11) [0.07-0.27]	0.009	0.41 (0.16) [0.10-0.40]	0.827	0.946
	After CPB	0.18 (0.05) [0.03-0.13]		0.39 (0.15) [0.09-0.36]		0.008
CPLLI	Before CPB	1.05 (0.01) [0.01-0.03]	0.616	1.04 (0.03) [0.02-0.08]	0.735	0.474
	After CPB	1.05 (0.02) [0.01-0.04]		1.05 (0.02) [0.01-0.04]		0.869
CPPLI	Before CPB	5.11 (0.90) [0.56-2.21]	0.013	5.14 (0.67) [0.41-1.64]	0.773	0.948
	After CPB	3.47 (0.53) [0.33-1.31]		5.02 (0.46) [0.29-1.12]		<0.001

Coefficient of microviscosity and polarity of erythrocyte membranes at the observation stages in CPB + CA and CPB + CA + NO groups						
Variables	Stages	CPB + CA group	P (between the stages of before and after CPB)	CPB + CA + NO group	P (between the stages of before and after CPB)	P (between groups)
CMLLI	Before CPB	0.29 (0.11) [0.07-0.26]	0.946	0.30 (0.09) [0.05-0.21]	0.451	0.821
	After CPB	0.28 (0.06) [0.04-0.15]		0.28 (0.04) [0.03-0.11]		0.799
CMPLI	Before CPB	0.40 (0.09) [0.06-0.24]	0.049	0.39 (0.08) [0.05-0.19]	0.946	0.847
	After CPB	0.24 (0.05) [0.03-0.11]		0.39 (0.09) [0.06-0.23]		0.019
CPLLI	Before CPB	1.05 (0.03) [0.02-0.08]	0.882	1.05 (0.03) [0.02-0.08]	0.864	0.954
	After CPB	1.05 (0.02) [0.01-0.04]		1.05 (0.01) [0.01-0.04]		0.727
CPPLI	Before CPB	4.62 (1.07) [0.67-2.63]	0.022	4.51 (0.93) [0.58-2.27]	0.624	0.846
	After CPB	2.86 (0.56) [0.35-1.37]		4.6 (0.84) [0.52-2.05]		0.002

Data expressed as mean (standard deviation) [95% confidence interval]. CA=circulatory arrest, CMLLI=coefficient of microviscosity in the areas of lipid-lipid interactions, CMPLI=coefficient of microviscosity in the areas of protein-lipid interactions, CPB=cardiopulmonary bypass, CPLLI=coefficient of polarity in the areas of lipid-lipid interactions, CPPLI – coefficient of polarity in the areas of protein-lipid interactions, i-FABP=intestinal enterocyte fatty acid binding protein, NO=nitric oxide

and, accordingly, on blood rheological properties and organ perfusion, including intestines. The defaecation rate was greater in groups with NO than in groups without NO, indicating better bowel function.

Ischaemia-reperfusion injury was confirmed by i-FABP, demonstrating less pronounced intestinal injury in NO groups during CPB and CA. Our findings fit into the concept of the effect of NO on splanchnic blood flow since NO is an important vasodilator that plays a central role in regulating organ perfusion.^[6] Other studies on i-FABP have already shown that during haemolysis, the release of free haemoglobin causes intravascular NO absorption, which leads to impaired organ perfusion with subsequent tissue injury and increased i-FABP levels.^[7-11]

To assess cellular energy reserves and mitochondrial functional state, we examined ATP and lactate concentrations in intestinal biopsies 1 h after CPB. All groups had a high lactate concentration, indicating increased anaerobic pathways during CPB and CA. ATP concentration in intestinal biopsies was higher in the CPB + NO group than in the CPB group, which may indicate better ATP-related mitochondrial respiration, possibly reducing the effect of oxidative

stress on the mitochondrial respiratory chain. The ATP concentration did not differ significantly in the CPB + CA + NO group compared to the CPB + CA group, likely due to more aggressive damage factors associated with non-perfusion CA.

To find the correlation between improved intestinal perfusion and NO effects, we also assessed the polarity and microviscosity of erythrocyte membranes, which indicate their deformability.^[12,13] The ability of erythrocytes to deform is a key factor in maintaining normal blood circulation, ensuring the passage of erythrocytes through the narrow capillaries of the microvasculature, thereby improving oxygen delivery to tissues.^[12-14]

After weaning from CPB, groups without NO showed a significant decrease in CMPLI and CPPLI, which indicates a deterioration in erythrocyte deformability after CPB.^[10,11] In the groups with NO, the same variables remained in the same range before and after CPB. This indicates the positive effect of NO on stabilising the structural organisation of protein-lipid interactions of erythrocyte membranes and maintaining better erythrocyte deformability. Our findings are also consistent with the study of

Bor-Kucukatay *et al.*, which showed that NO is an important factor in erythrocyte mechanical behaviour and plays a regulatory role in maintaining normal erythrocyte deformability.^[6,13,15] Perhaps that is why ischaemia–reperfusion injury was less pronounced in histological samples in groups with NO, and the plethora and dilated vessels of the small intestinal villi only confirm the effect of NO as a vasodilator and a substance that is involved in the regulation of splanchnic blood flow.^[1,6,16]

The damaged lipid and protein components lead to impaired erythrocyte deformability, a decrease in its ability to penetrate small capillaries and diffuse gases and, consequently, tissue hypoxia.^[10,11,14] It is possible that NO, under increased oxidative stress during CPB, CA, and hypothermia, can prevent the active formation of reactive oxygen species and lipid peroxidation and, consequently, reduce damage to membrane structures by free radicals.^[12,13,17]

We proved that NO has a positive effect on the intestine, improving its perfusion and functional state and reducing damage. Such effects are useful in clinical practice, especially in aortic surgery, since the intestine and other organs are target organs of ischaemia–reperfusion injury. Perioperative use of Tianox in the future can reduce the risks and incidence of postoperative complications and the duration of intensive care unit and in-hospital stay, thereby cutting costs for treating patients. This technique is promising and requires further clinical research.

CONCLUSION

When modelling CPB and CA, NO delivery leads to improved intestinal functional status, decreased expression of biomarkers of damage, optimised energy metabolism and reduced morphological signs of damage in intestinal cells. The delivery of NO also has a positive effect on the structural organisation of erythrocyte membranes, improving their deformability.

Study data availability

De-identified data may be requested with reasonable justification from the authors (email to the corresponding author) and shall be shared upon request.

Acknowledgement

We express our gratitude to Elena Kim for her help in the editing of the manuscript.

Financial support and sponsorship

This research was performed in the framework of the state assignment for basic research (theme no. 122123000017-3) entitled ‘Organ protection with nitric oxide in cardiovascular surgery: technological support (synthesis and delivery devices), mechanisms for implementing the protective effects and impact on clinical outcomes’.

Conflicts of interest

There are no conflicts of interest.

ORCID

Nikolay O. Kamenshchikov: <https://orcid.org/0000-0003-4289-4439>

Elena A. Churilina: <https://orcid.org/0000-0003-3562-9979>

Irina V. Sukhodolo: <https://orcid.org/0000-0001-9848-2068>

Vyacheslav A. Korepanov: <https://orcid.org/0000-0002-2818-1419>

Tatiana Yu. Rebrova: <https://orcid.org/0000-0003-3667-9599>

Boris N. Kozlov: <https://orcid.org/0000-0002-0217-7737>

REFERENCES

1. Wu MY, Yiang GT, Liao WT, Tsai AP, Cheng YL, Cheng PW, *et al.* Current mechanistic concepts in ischemia and reperfusion injury. *Cell Physiol Biochem* 2018;46:1650-67.
2. Mc Loughlin J, Hinchion J. The gut microbiome and cardiac surgery are unusual symphony. *Perfusion* 2023;38:1330-9.
3. Mu K, Yu S, Kitts DD. The role of nitric oxide in regulating intestinal redox status and intestinal epithelial cell functionality. *Int J Mol Sci* 2019;20:1755. doi: 10.3390/ijms20071755
4. Kamenshchikov NO, Anfinogenova YJ, Kozlov BN, Svirko YS, Pekarskiy SE, Evtushenko VV, *et al.* Nitric oxide delivery during cardiopulmonary bypass reduces acute kidney injury: A randomised trial. *J Thorac Cardiovasc Surg* 2022;163:1393-403.
5. Kamenshchikov NO, Mandel IA, Podoksenov YK, Svirko YS, Lomivorotov VV, Mikheev SL, *et al.* Nitric oxide provides myocardial protection when added to the cardiopulmonary bypass circuit during cardiac surgery: Randomized trial. *J Thorac Cardiovasc Surg* 2019;157:2328-36.
6. LoBue A, Heuser SK, Lindemann M, Li J, Rahman M, Kelm M, *et al.* Red blood cell endothelial nitric oxide synthase: A major player in regulating cardiovascular health. *Br J Pharmacol* 2023. doi: 10.1111/bph. 16230
7. Zvyagin AA, Bavykina IA, Nastaushcheva TL, Bavykin DV. Intestinal fatty acid binding protein is the promising marker of small intestine permeability. *Rossiyskiy Vestnik Perinatologii i Peditrii* (Russian Bulletin of Perinatology and Pediatrics) 2020;65:29-33. (In Russ.).
8. Straarup D, Gotschalck KA, Christensen PA, Krarup H, Lundbye-Christensen S, Handberg A, *et al.* Exploring I-FABP, endothelin-1 and L-lactate as biomarkers of acute intestinal necrosis: A case-control study. *Scand J Gastroenterol* 2023;58:1359-65.

9. Seethaler B, Basrai M, Neyrinck AM, Nazare JA, Walter J, Delzenne NM, *et al.* Biomarkers for assessment of intestinal permeability in clinical practice. *Am J Physiol Gastrointest Liver Physiol* 2021;321:G11-7.
10. McNamee AP, Simmonds MJ. Red blood cell sublethal damage: hemocompatibility is not the absence of hemolysis. *Transfus Med Rev* 2023;37:150723. doi: 10.1016/j.tmr. 2023.03.001
11. Wang S, Griffith BP, Wu ZJ. Device-induced hemostatic disorders in mechanically assisted circulation. *Clin Appl Thromb Hemost* 2021;27:1076029620982374. doi: 10.1177/1076029620982374
12. Kobayashi J, Ohtake K, Murata I, Sonoda K. Nitric oxide bioavailability for red blood cell deformability in the microcirculation: A review of recent progress. *Nitric Oxide* 2022;129:25-9.
13. Kuhn V, Diederich L, Keller TCS 4th, Kramer CM, Lückstädt W, Panknin C, *et al.* Red blood cell function and dysfunction: Redox regulation, nitric oxide metabolism, anemia. *Antioxid Redox Signal* 2017;26:718-42.
14. Li N, Chen S, Xu K, He MT, Dong MQ, Zhang QC, *et al.* Structural basis of membrane skeleton organisation in red blood cells. *Cell* 2023;186:1912-29.e18.
15. Bor-Kucukatay M, Wenby RB, Meiselman HJ, Baskurt OK. Effects of nitric oxide on red blood cell deformability. *Am J Physiol Heart Circ Physiol* 2003;284:H1577-84.
16. Leo F, Suvorava T, Heuser SK, Li J, LoBue A, Barbarino F, *et al.* Red blood cell and endothelial eNOS independently regulate circulating nitric oxide metabolites and blood pressure. *Circulation* 2021;144:870-89.
17. Diederich L, Suvorava T, Sansone R, Keller TCS 4th, Barbarino F, Sutton TR, *et al.* On the effects of reactive oxygen species and nitric oxide on red blood cell deformability. *Front Physiol* 2018;9:332. doi: 10.3389/fphys.2018.00332

THE METHOD OF DELIVERING NO TO THE CIRCUIT OF THE VENTILATOR AND TO THE CPB CIRCUIT

Figure 1 (a and b) shows two diagrams illustrating NO delivery and NO/NO₂ monitoring during the study.

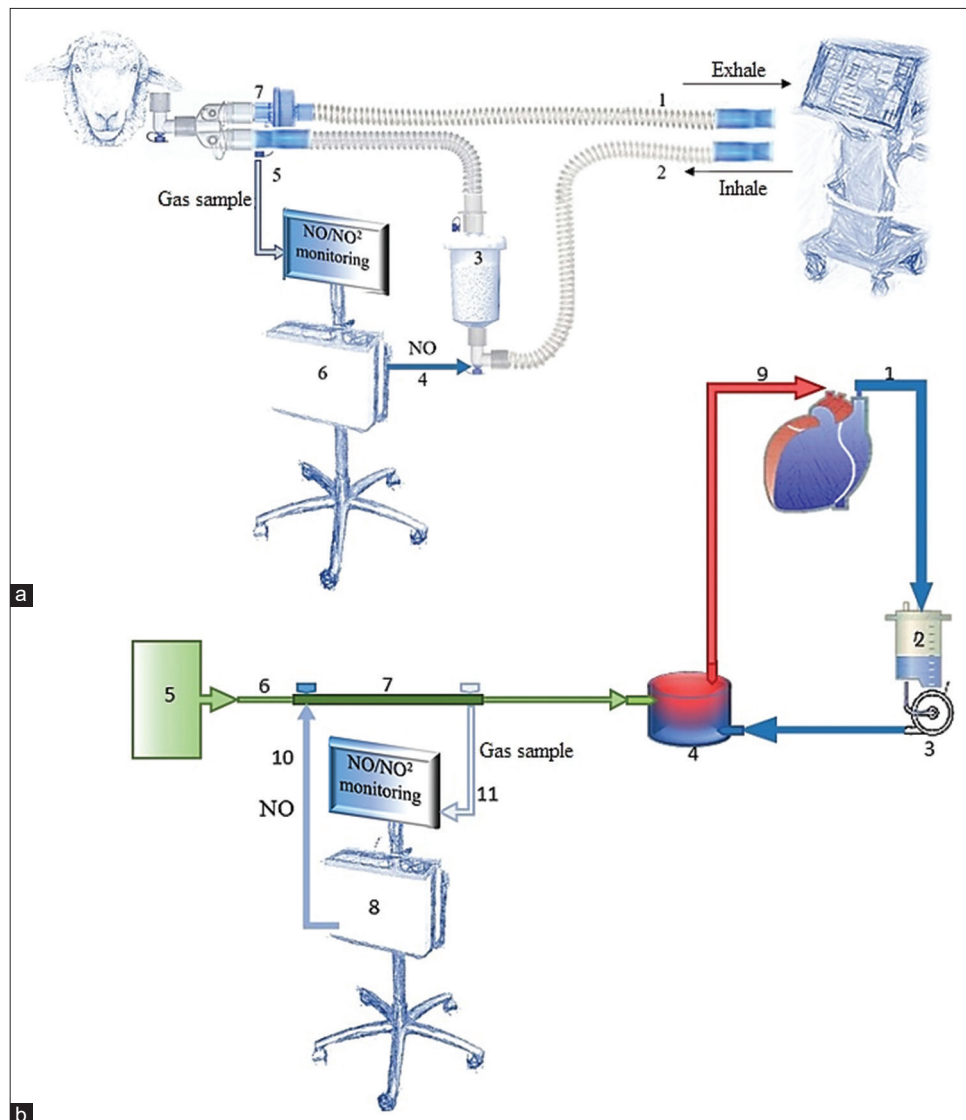


Figure 1: (a) Scheme of NO delivery through the ventilator circuit: 1 — exhale; 2 — inhale; 3 — absorber; 4 — NO delivery to the inhalation hose; 5 — gas sample; 6 — experimental device for a plasma-chemical synthesis of nitric oxide; 7 — hydrophobic virus-bacterial filter. (b) Scheme of NO delivery through the CPB machine circuit: 1 — venous line; 2 — cardiomy reservoir; 3 — roller pump; 4 — oxygenator; 5 — gas blender; 6 — gas flow; 7 — 2 in-line adapters ¼ with Luer connector; 8 — experimental device for a plasma-chemical synthesis of nitric oxide; 9 — arterial line; 10 — NO delivery; 11 — gas sample

Nitric oxide delivery: For NO delivery, we used a special device for a plasma-chemical NO synthesis AIT-NO-01 (“Tianox”) manufactured by the Russian Federal Nuclear Center - All-Russian Research Institute of Experimental Physics (RFNC-VNIIEF, Rosatom State Corporation enterprise, Sarov, Russia), which supplied inhaled NO and monitored the delivered NO/NO₂ in the gas-air mixture supply line during the study. The NO concentration in “CPB+NO” and “CPB+CA+NO” groups was 80 ppm. The maximum permissible NO₂ concentration in the “CPB+NO” and “CPB+CA+NO” groups was considered 2 ppm. Experimental animals from “CPB” and “CPB+CA” groups received a standard oxygen-air mixture without NO. To ensure safety, the concentrations of delivered NO/NO₂ and methemoglobin (MetHb) levels in the blood were continuously monitored with Stat Profile pHox Ultra analyser (Nova Biomedical, USA) during the study.

ANAESTHESIA AND CARDIOPULMONARY BYPASS TECHNIQUE

The experiment in all groups began with mask induction of anaesthesia with sevoflurane. Upon reaching the target level of anaesthesia, the animal was placed in the left lateral position and secured with soft bands. After this, the surgical field was shaved and treated. Next, under aseptic conditions, catheterization of the great saphenous vein of the hind limb was performed with an 18 G catheter for infusion therapy and induction of anaesthesia. Infusion therapy was carried out with a solution of Sodium chloride 0.9%. Premedication included atropine sulfate 0.5 mg and chloropyramine 20 mg. Before induction of anaesthesia, standard monitoring was established: pulse oximetry, ECG (electrodes were placed in skin incisions on the anterior-lateral surface of the body). Next, induction anaesthesia was performed with fractional injections of propofol 1% until signs of anaesthesia appeared, after which, against the background of spontaneous breathing, direct laryngoscopy was performed, followed by orotracheal intubation with endotracheal tube (ETT) – Size 6.5. After assessing the adequacy of the placement of the ETT in the trachea and effective ventilation (visually - the presence of symmetrical bilateral excursions of the chest, auscultation - the presence of breathing sounds on both sides), the tube was fixed and mechanical ventilation was started using the Puritan Bennett 760 (USA) device using a modified breathing circuit in the Controlled Mandatory Ventilation (CMV) with controlled volume: tidal volume 8 ml/kg and respiratory rate 20 per minute, fractional oxygen concentration in the inhaled mixture (FiO₂) 0.5, positive end-expiratory pressure 5 cmH₂O. Sheep from “CPB+NO” and “CPB+CA+NO” groups received NO immediately after tracheal intubation through a modified ventilator circuit. For the synthesis, delivery and monitoring of NO/NO₂, a device for plasma-chemical synthesis of NO was used. Throughout the experiment, propofol 5 mg/kg/h was infused to maintain anaesthesia, and pipecuronium bromide 0.1 mg/kg was administered to provide neuromuscular blockade. Extended monitoring during the experiment included: ECG, invasive measurement of blood pressure (BP), pulse oximetry, capnography, diuresis and thermometry using the Nihon Kohden Life Scope I BSM-2301 K monitoring system (Nihon Kohden, Japan) with the installation of a temperature sensor in the esophagus, and in groups with CA, a temperature sensor was additionally installed in the rectum.

For the purpose of invasive measurement of BP and collection of blood samples for laboratory analysis of blood gas composition, the common carotid artery was surgically harvested and catheterized with 20 G catheter. The blood gas composition, as well as the MetHb level, were determined using the STAT PROFILE Critical Care Xpress device (Nova Biomedical, USA). For infusion therapy, inotropic and vasopressor support, the internal jugular vein was cannulated with a double lumen catheter 7 F. After catheterization of the vessels, a right thoracotomy was performed along the 4th intercostal space. CPB was performed using a CPB machine Maquet HL 20 (Maquet, Germany). The CPB machine was connected according to the “aorta – superior vena cava – inferior vena cava” scheme. During CPB, the perfusion index was 2.5 L/min/m². Mean BP during CPB was maintained at 50–60 mmHg. In groups without CA, CPB was performed under normothermia, maintaining esophageal temperature at 36–36.6°C. In two groups with CA, upon reaching the esophageal temperature of 30°C, occlusion of the thoracic aorta was performed for 15 min. After 15 min, the thoracic aorta was unclamped followed by reperfusion, and warming to 36.6°C. The total CPB time in all groups was 90 min. To ensure hypocoagulation during CPB, heparin was used at a dose of 3 mg/kg intravenously, maintaining an activated clotting time (ACT) >450 s.

TECHNIQUE FOR ANALYZING THE OBTAINED ENDPOINTS

Determination of intestinal ischemia marker - i-FABP

I-FABP is an intestinal fatty acid binding protein that is expressed by mature enterocytes and is rapidly released into the bloodstream when they are damaged, and is a sensitive marker of intestinal mucosal injury.

To determine the concentration of intestinal ischemia marker, i-FABP, venous blood was collected before the start of CPB and after weaning from CPB. The obtained blood was centrifuged for 10 min at 3500 rpm, then frozen and stored in accordance with the manufacturer’s instructions, and as specimens accumulated, the intestinal fraction of the fatty acid binding protein i-FABP was determined using the enzyme-linked immunosorbent assay (Human I-FABP, Hycult Biotechnology) with SunRise absorbance reader (Tecan, USA).

Determination of ATP concentration in intestinal tissue biopsies

To determine the concentration of ATP in intestinal tissue biopsies 1 hour after CPB, intestinal tissue biopsies were taken, then they were frozen in liquid nitrogen. The resulting specimens were homogenized in liquid nitrogen and centrifuged for 10 min at 3000 rpm at a temperature of 2°C. Next, a supernatant liquid was obtained, which was collected, neutralized, and the specimen volume was adjusted to 2 ml. ATP determination was carried out using the ATP Bioluminescent Assay Kit on Lucy 2 luminometer.

The determination of ATP is based on the following reactions:

- 1) $\text{ATP} + \text{Luciferin} \rightarrow (\text{enzyme luciferase}) \text{Adenyl-luciferin} + \text{PPi}$;
- 2) $\text{Adenyl-luciferin} + \text{O}_2 \rightarrow \text{Oxyluciferin} + \text{AMP} + \text{CO}_2 + \text{light}$.

Reaction 1 is reversible, its equilibrium is shifted to the right; reaction 2 is irreversible, therefore the ATP content in the initial sample is the limiting factor of the reaction, and the amount of light released is directly proportional to the ATP concentration in the solution.

Determination of lactate concentration in intestinal tissue biopsies

To determine the concentration of lactate in intestinal tissue biopsies, intestinal tissue biopsies were taken 1 hour after CPB, then they were frozen in liquid nitrogen. The resulting specimens were homogenized in liquid nitrogen and centrifuged for 10 min at 3000 rpm at a temperature of 2°C; the resulting supernatant liquid was collected, neutralized, and the sample volume was adjusted to 2 ml. Lactate determination was carried out using the enzyme immunoassay method using the L-Lactate Assay Kit on Infinite 200 multifunctional microplate reader. The principle of this analysis is based on lactate oxidation, which is catalyzed by lactate dehydrogenase, so that the resulting NADH is reduced by formazan reagent. The color intensity of the product is proportional to the lactate concentration in the specimen.

Histology of intestinal tissue

During the surgical stage of anaesthesia, the animals were humanely removed from the experiment, followed by collection of material for morphological analysis. The material for morphological analysis is a fragment of the small intestine. For uniform fixation, a flat-shaped fragment of the small intestine measuring 1–2 cm by 3–5 mm was excised. After collecting the material, it was placed in a container with 10% neutral formaldehyde as a fixative. The ratio of the volume of material taken and the volume of fixative is 1:20. Then the material was stored at a temperature of +4, +6 °C until delivery to the pathology laboratory. Histological sections were prepared on a sled microtome (MS-1, manual, Russia) with a thickness of 5–7 μm . To analyze the morphological image, deparaffinized histological sections of organs were stained with hematoxylin-eosin according to the generally accepted technique to obtain review samples.

Determination of coefficient of microviscosity and polarity of erythrocyte membranes

To determine the coefficient of microviscosity and polarity of erythrocyte membranes, venous blood was taken before and after CPB.

Blood was collected into vacutainers containing lithium heparin (17 IU/ml) sprayed onto the walls. Blood samples were centrifuged at 1500 rpm for 10 min. After removal of plasma, the erythrocytes were washed 3 times with cooled saline, each time the erythrocytes were sedimented at 1500 rpm for 10 min. Erythrocyte membranes were obtained by hypoosmotic hemolysis. The content of total protein in the suspension of erythrocyte shadows was determined by Micro Lowry method modified by Ohnishi S.T. using Sigma reagents. To determine the spectral characteristics, a sample of erythrocyte membranes was diluted in 10 mM Tris-HCl buffer (pH = 7.4) to a final protein concentration of 0.3 mg/ml.

The spectral characteristics of membrane interactions with pyrene fluorescent probe (Sigma) were determined on Cary Eclipse fluorescence spectrometer i (Varian, USA). 20 μl of a 10 μM alcohol solution of the pyrene probe was added to 2 ml of erythrocyte membrane suspension. The microviscosity properties of membranes in the region of annular and total lipids were assessed by the degree of pyrene excimerization calculating the ratio of fluorescence intensity of excimers and monomers (J470/J370) at an excitation wavelength (λ_b) of 285 and 340 nm, respectively. Polarity was analyzed by the ratio of the amplitudes of vibration peaks of excimers and monomers (J390/J370) at excitation wavelengths (λ_b) 285 and 340 nm, respectively.